Testing Of New Imaging Algorithm For Segmented MR Images Of Breast Tissue

Michael V. Klibanov*, Thomas R. Lucas*, Robert M. Frank*, Randall L. Barbour+, and Harry L. Graber+

*Department of Mathematics, University of North Carolina at Charlotte, Charlotte, NC 28223, U.S.A.

+Department of Pathology, SUNY Health Science Center at Brooklyn, 450 Clarkson Ave., Brooklyn, NY 11203, U.S.A.

Abstract

In a paper by the first three authors a new algorithm for Optical Tomography (OT) in the time domain was described and tested for the case of an uniform background medium (see current proceedings). The goal of this paper is to test this method for the case where the background medium is an anatomically accurate optical map of the breast tissue obtained on the basis of a segmented Magnetic Resonance (MR) image. The key innovation of this imaging algorithm lies in a new approach for a novel linearized problem (LP). Such an LP is reduced to a boundary value problem for a coupled system of elliptic partial differential equations, rather than a conventional form of an ill-posed integral equation. The solution of this system in turn is done very rapidly. Thus, this is a fast imaging algorithm.

Key Words. MR image, breast cancer diagnosis, optical tomography, elliptic systems method

1. Introduction

In the past several years many researchers have been working on numerical methods which would solve the problem of optical imaging of small inclusions hidden in turbid media, such as biological tissues, for example, c.f. [1-3,7]. This challenging problem inevitably leads to a very difficult mathematical Inverse Scattering Problem (ISP) either for the transport or diffusion equation. Generally, this field of study is called Diffusion Tomography, or Optical Tomography (OT). One of most important medical applications of OT is for early diagnosis of breast cancer.

In the majority of publications on this subject the resulting inverse problem is reduced to an ill-posed integral equation, c.f. [1-3,8]. The solution of such an equation is a time consuming procedure. In addition, these methods require the pre-computation of the Green's function, which is also time consuming. In [5] a novel imaging algorithm was presented. The *core* of this numerical method consists in a novel approach for a new LP. Namely, a new LP is derived and reduced to a well-posed boundary value problem for a system of elliptic partial differential equations (PDEs). On the other hand, the classical theory of numerical methods for PDEs implies that, unlike an *integral* equation, solution of a well posed boundary value

SPIE Vol. 2979 • 0277-786X/97/$10.00

problem for a partial *differential* equation amounts to the factorization of a well-conditioned, sparse matrix (few non-zero entries). This in turn can be done very rapidly by conventional methods [4]. Hence, a strong advantage of this technique is its *speed.*

In this paper we present results of tests of the method [5] for the case of an anatomically accurate optical map of breast tissue obtained on the basis of a segmented MR image. We consider the case of time dependent data. The ESM can be extended to other data collection schemes [5,6], but corresponding numerical results have not yet been obtained.

As in [5], we consider the forward problem for the diffusion equation in the whole euclidian space R^n, $n = 2, 3$. This scenario reflects the suggestion of immersing the breast in a larger balloon whose optical properties would be about the same as those of the breast tissue [2]. We will consider only a *single* location of the light source x_0. In a practical scenario this would lead to an essential reduction in the acquisition time, as compared with conventional cases requiring many sources.

Suppose light is radiated by an ultrafast laser pulse and propagates in a turbid media. Photons propagating through such a media experience many random scattering events and their propagation is governed by the diffusion equation. The forward problem for this equation consists in determining the light intensity $u(x,t)$ satisfying

$$\begin{aligned} u_t &= \text{div}\ (D(x)\nabla u) - a(x)u,\ x \in R^n,\ n = 2,3;\ t \in (0,T), \\ u|_{t=0} &= \delta(x - x_0) \end{aligned} \tag{1.1}$$

Assuming isotropic scattering, let $\mu_s(x)$ and $\mu_a(x)$ be the scattering and absorption coefficients respectively. We also assume that the media is low absorbing with $\mu_a \ll \mu_s$ (such as is the case for biological tissues, for example). Let c be the speed of light in the media. Then the diffusion coefficient $D(x)$ and the absorption term $a(x)$ are [7]

$$D(x) = \frac{c}{\mu_s(x)} \text{ and } a(x) = c\mu_a(x)$$

Cancerous tumors absorb light more than the surrounding tissues (i.e., the reference medium). To find these tumors, one should find those regions where the values of the absorption coefficient $a(x)$ are different from those of the reference medium. In addition, the optical properties of the reference medium are usually not known very accurately. Hence, one should also "correct" the initial guess about the background medium. Thus, one should solve an ISP for the equation (1.1). Let $\Omega \subset R^n\,(n = 2,3)$ be a bounded domain of interest with a piecewise smooth boundary $\partial\Omega$. Let $\{x_i\}_{i=1}^m \subset \partial\Omega$ be a set of detectors placed around $\partial\Omega$. If one is measuring the function $u(x_i,t)$ at these detectors, then one can interpolate these readings over the entire boundary $\partial\Omega$. Thus the inverse problem is stated as follows:

Inverse Problem. *Let the function $a(x)$ be given outside of Ω, and be approximated by $a(x) = a_0(x) + h(x)$ inside of Ω, where the function $a_0(x)$ is known everywhere ($a_0(x)$ describes properties of the background medium), $h(x)$ is a small unknown perturbation of $a_0(x)$; and $h(x) = 0$ for $x \in R^n \backslash \Omega$. Determine the function $h(x)$ assuming that the intensity $\varphi(x,t)$ at the boundary is given,*

$$u = \varphi(x,t),\ \text{for } x \in \partial\Omega,\ t \in (T_0, T_F),$$

where (T_0, T_F) *is a subinterval of the time interval* $(0,T)$ *and* $T_0 > 0$.

As it was shown in [5], given the intensity $\varphi(x,t)$, one can uniquely determine flux at the boundary, i.e. the function $\frac{\partial u}{\partial \nu}|_{\partial\Omega\times(T_0,T_F)} = \psi(x,t)$, and vice versa. Here ν is the unit normal vector on $\partial\Omega$ pointing outside of Ω . Therefore, we will always assume below that the following two functions $\varphi(x,t)$ and $\psi(x,t)$ are given

$$u|_{\partial\Omega\times(T_0,T_F)} = \varphi(x,t), \ \frac{\partial u}{\partial \nu}|_{\partial\Omega\times(T_0,T_F)} = \psi(x,t)$$

2. Outline Of The Elliptic Systems Method

In this section we briefly outline the ESM, referring details to [5]. Let the function $u_0(x,t)$ be the solution of the Cauchy problem (1.1) for the background medium, which is not necessarily homogeneous,

$$u_{0t} = \text{div}\ (D(x)\nabla u_0) - a_0(x)u_0, \quad u_0(x,0) = \delta(x-x_0). \tag{3.1}$$

Let $v = u - u_0$. Linearizing the equation for the function v with respect to the perturbation function $h(x) = a(x) - a_0(x)$, we obtain

$$v_t = \text{div}\ (D\nabla v) - a_0(x)v - h(x)u_0, \quad v(x,0) = 0. \tag{3.2}$$

As the first step, we *eliminate* the function $h(x)$ from (3.2). In doing this we use the fact that $\partial/\partial t[h(x)] \equiv 0$. First, we isolate $h(x)$ in (3.2) dividing both sides of this equation by $u_0(x,t)$. Let

$$H(x,t) = \frac{v}{u_0} = \frac{u}{u_0} - 1. \tag{3.3}$$

Substituting $v = u_0 H$ into (3.2) and using (3.1), we obtain

$$H_t = \text{div}\ (D(x)\nabla H) + 2D(x)\frac{\nabla u_0}{u_0}\nabla H - h(x) \tag{3.4}$$

Introduce the derivative $p(x,t) = H_t(x,t)$ of the function H. Likewise, we can prove that the initial condition for the function H is $H(x,0) = 0$. Differentiating the equation (3.4) with respect to t, we eliminate $h(x)$ and obtain a new integro-differential equation for the function $p(x,t)$,

$$p_t - \text{div}\ (D(x)\nabla p) - 2D\frac{\partial}{\partial t}\left[\frac{\nabla u_0}{u_0}\int_0^t \nabla p(x,\tau)\,d\tau\right] = 0 \tag{3.5}$$

In addition, (2.3) leads to

$$p|_{\partial\Omega\times(T_0,T_F)} = \varphi_1(x,t), \ \frac{\partial p}{\partial \nu}|_{\partial\Omega\times(T_0,T_F)} = \psi_1(x,t), \tag{3.6}$$

$$\text{where } \varphi_1(x,t) = \frac{\partial}{\partial t}\left(\frac{\varphi}{u_0}\right) \text{ and } \psi_1(x,t) = \frac{\partial}{\partial t}\left[\frac{\psi}{u_0} - \frac{\varphi}{u_0^2}\frac{\partial u_0}{\partial \nu}\right] \tag{3.7}$$

Should the function p be computed, then the perturbation $h(x)$ will be reconstructed as

$$h(x) = \frac{1}{T_0 - T_F} \int_{T_0}^{T_F} \left[\text{div } (D(x) \nabla H) + 2D \frac{\nabla u_0}{u_0} \nabla H - H_t \right] dt,$$
$$\text{where } H(x,t) = \int_0^t p(x,\tau) d\tau$$

We take the average value in the integral for h because the integrand might depend on t in practical computations.

Therefore, the *central point* of further considerations should consist in the finding of the function $p(x,t)$. Let $\{a_k(t)\}_{k=1}^{\infty}$ be an orthonormal basis in the Hilbert space $L_2(T_0, T_F)$, such that all functions $a_k(t)$ are real valued and analytic as functions of the real variable t for $t > 0$. A good example is the system of Legendre polynomials. We assume that the function $p(x,t)$ can be represented as a finite generalized Fourier series with respect to t, as

$$p(x,t) \approx \sum_{k=1}^{N} a_k(t) \; Q_k(x), \text{ for } (x,t) \in \Omega \times (0, T_F),$$

where $N \geq 1$ is an integer and the functions $Q_k(x)$ are generalized Fourier coefficients of the function p over the interval (T_0, T_F),

$$Q_k(x) = \int_{T_0}^{T_F} p(x,t) \; a_k(t) \, dt.$$

Now we want to obtain a coupled elliptic system with respect to the functions $Q_k(x)$. First, consider boundary conditions for these functions on $\partial\Omega$.

Denote $\alpha(x) = (\alpha_1(x), ..., \alpha_N(x))$, $\beta(x) = (\beta_1(x), ..., \beta_N(x))$ for $x \in \partial\Omega$, where

$$\alpha_k(x) = \int_{T_0}^{T_F} \varphi_1(x,t) \, a_k(t) \, dt, \quad \beta_k(x) = \int_{T_0}^{T_F} \psi_1(x,t) \, a_k(t) \, dt, \text{ for } 1 \leq k \leq N. \tag{3.8a}$$

Note that by (3.7) the functions α_k and β_k can be computed as

$$\alpha_k(x) = \frac{\varphi}{u_0} a_k \Big|_{T_0}^{T_F} - \int_{T_0}^{T_F} \frac{\varphi}{u_0} a_k'(t) \, dt \tag{3.8b}$$

$$\beta_k(x) = \left[\frac{\psi}{u_0} - \frac{\varphi}{u_0^2} \frac{\partial u_0}{\partial \nu} \right] a_k \Big|_{T_0}^{T_F} - \int_{T_0}^{T_F} \left[\frac{\psi}{u_0} - \frac{\varphi}{u_0^2} \frac{\partial u_0}{\partial \nu} \right] a_k'(t) \, dt \tag{3.8c}$$

Formulas (3.8b,c)are more convenient for practical computations than (3.8a), since they do not require the differentiation of the data φ & ψ, which are given with noise. The derivatives $a_k'(t)$, on the other hand, are trivial to calculated explicitly.

Also, introduce the N-dimensional vector valued function $Q(x) = (Q_1(x), ..., Q_N(x))$. Multiply both sides of (3.5) by $a_k(t)$ for $k = 1, ..., N$, and integrate with respect to t over (T_0, T_F). We obtain the following boundary value problem for a coupled elliptic system of PDEs

$$A(Q) := \text{div } (D \nabla Q) - \sum_{j=1}^{n} B_j(x) \frac{\partial Q}{\partial x_j} - CQ = 0 \tag{3.9a}$$

$$Q|_{\partial\Omega} = \alpha(x)\,,\ \frac{\partial Q}{\partial \nu}|_{\partial\Omega} = \beta(x) \tag{3.9b}$$

where the $N \times N$ matrices B_j depend on the function u_0, and elements of the $N \times N$ matrix C are

$$c_{ks} = \int_{T_0}^{T_F} a_s'(t)\ a_k(t)\,dt;\quad k, s = 1, ..., N.$$

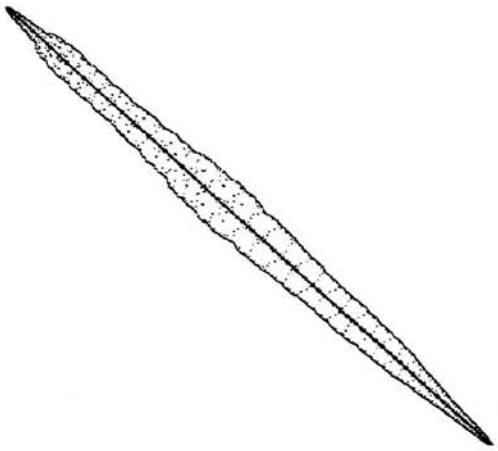

Figure 1. Typical Matrix Structure In Inverse Solver

Because of the *differential*, rather than conventional *integral* form of the resulting system (3.9), the solution of this system by the Finite Element Method (FEM) amounts to the factorization of *sparse, well-conditioned* matrices with non-zero entries clustered along the diagonal, c.f. [4]. A typical matrix structure for our inverse solver is displayed on Fig. 1. Dots denote non-zero 2×2 submatrices. This should lead to very rapid solution times, which is the *key advantage* of this imaging algorithm. An approach to solving the boundary value problem (3.9) through the solution of an associated self-adjoint 4th order elliptic system was described in [5].

3. Numerical Tests

The resulting 4th order boundary value problem [5] was solved by the Finite Element Method (FEM), using modifications of an existing FEM code FESOP (Finite Element Solution of PDE's) outlined in [7]. The use of the very convenient mesh generation software included in this code enables one to put additional mesh in the regions where the inclusions are "suspected" to be located. That is, one first uses a uniform mesh in the inverse solver and locates the inclusions approximately. Next, one adds additional mesh in "suspected" regions and repeats the use of the inverse solver. In our code functions $a_k(t)$ are Legendre polynomials. So far we have found that the best choice of the number N of these polynomials (=the number of equations in the elliptic system) is $N \leq 3$. Usually, the images degrade for $N \geq 4$.

We have also introduced multiplicative Gaussian random noise in the data for all detectors on $\partial\Omega$ with a standard deviation of σ. Let ξ be a Gaussian random variable with the mathematical expectation 0 and standard deviation σ. Then with 95% probability $|\xi| < 2\sigma$. Hence the *noise level* can be taken to be 2σ. In the tests below we use $\sigma = 0.01$ Thus, noise is at the 2% level. Since the flux on $\partial\Omega$ can be determined as the solution of a boundary value problem given the intensity on $\partial\Omega$ and vice versa, we introduced the noise in just one of flux or intensity (also, see Remark in the end of section 2 of [5]). Next, we smoothed this noise by the least square interpolation of noisy temporal profiles by Legendre polynomials over a somewhat larger interval (T', T''), where $0 < T' \leq T_0 < T_F \leq T''$ and used formulas (3.8b,c) to compute the boundary data for functions $Q_k(x)$ using smooth values of φ/u_0.

Tests were conducted on a Silicon Graphics Indigo (SGI) with one processor. In all of these tests the starting point of the ESM was the absorption coefficient $a_0(x)$ of the background medium. Our images display the function $h(x)$, the correction term. Our code iterates the solution as follows. Given the vector valued function Q,the code readily updates a_0 as $a_0(x) := a_0(x) + h(x)$. Next, it solves the Cauchy problem (1.1) with $a = a_0$ and updates the boundary conditions at the detectors.

We used an anatomically accurate optical map of a female breast, which was obtained on the basis of segmented Magnetic Resonance Images (MRI) [2]. Fig. 2 displays the MRI cross-section within the square Ω of $192mm \times 192mm$. The size of the MRI cross-section was $120mm \times 72mm$ [2]. The rest of the plane outside of this cross-section was "filled" with parenchyma and in the whole plane $\mu_s \equiv 0.5mm^{-1}$. This scenario reflects a well known suggestion to immerse the breast into a scattering medium of a large size in order to avoid imposing ambiguous boundary conditions on the breast's surface. The total number of detectors was 52. They were uniformly distributed over four sides of the square Ω. The unique light source was located in the middle of the left side of the square Ω. The time interval on which we analyzed the data was $(T_0, T_F) = (1557, 2830)ps$, and the data was smoothed on the interval $(T', T'') = (1415, 3538)ps$ using 300 data points.

We also introduced two small "tumors" which are shown as accurate small disks on Fig. 2. Diameters of the tumors were $3.8mm$. "The breast was segmented into two different tissue types - fat and parenchyma [2]". The bulk of the MRI cross-section is fat. We have imaged the function $\mu_a(\vec{x})$. We took $c = 0.225mm/ps$; and the absorption coefficients were as in [5]: $\mu_a(\vec{x}) = 0.01\ mm^{-1}, \mu_a(\vec{x}) = 0.03\ mm^{-1}$, and $\mu_a(\vec{x}) = 0.06\ mm^{-1}$ for parenchyma, fat, and tumors respectively. Thus, the absorption contrast tumors/parenchyma (the bulk of the medium) is 2:1, which is very *low*.

Test #1. In this test we introduced the above noise in the intensity readings. We took $N = 3$ on the first iteration of the ESM, and we used $N = 1$ on two additional iterations (3 iterations total). The first iteration of the ESM gave a pretty good guess about the locations of "tumors" (not shown). The CPU time was: 1.3 minutes for the forward solver and 12 seconds for the inverse solver with 1024 finite elements, which is almost real time. Next, we added 300 additional finite elements (1324 total) in two spots were inclusions where "suspected" to be located and repeated the inverse run again. This run took 40 seconds of CPU time (for $N = 3$). Two additional iterations of the ESM were performed in order to improve the locations of the inclusions and to eliminate artifacts (similarly to [5]). For these additional runs we took the number of equations in the system (3.9) to be $N = 1$ (1324 finite

elements for the inverse solver). The CPU time for the inverse tun was 5 seconds on each of these iterations. Figure 3 displays the resulting image obtained after three iterations of the ESM in 4 minutes *total* CPU time with no pre-computations. The locations of the inclusions where imaged accurately. The 3-Dimensional view of this image is shown on Figure 4.

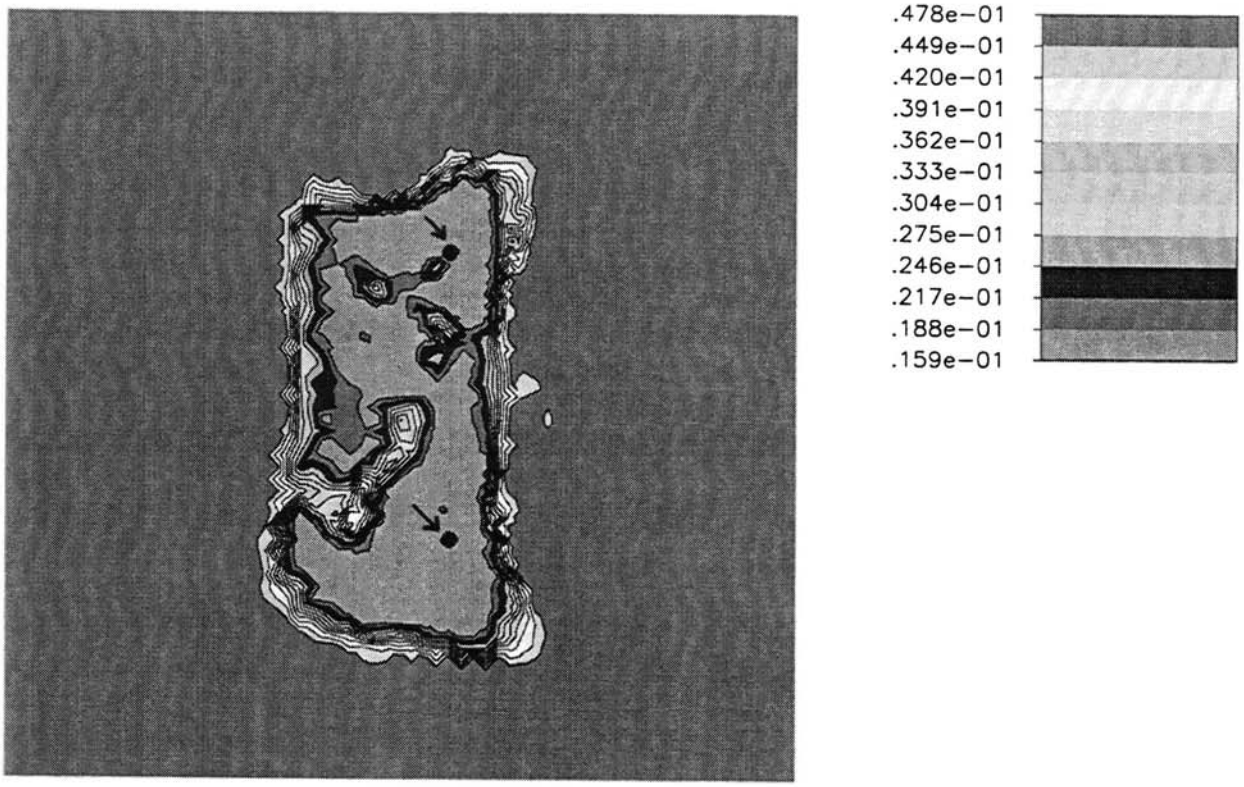

Figure 2. MRI cross-section with "tumors"

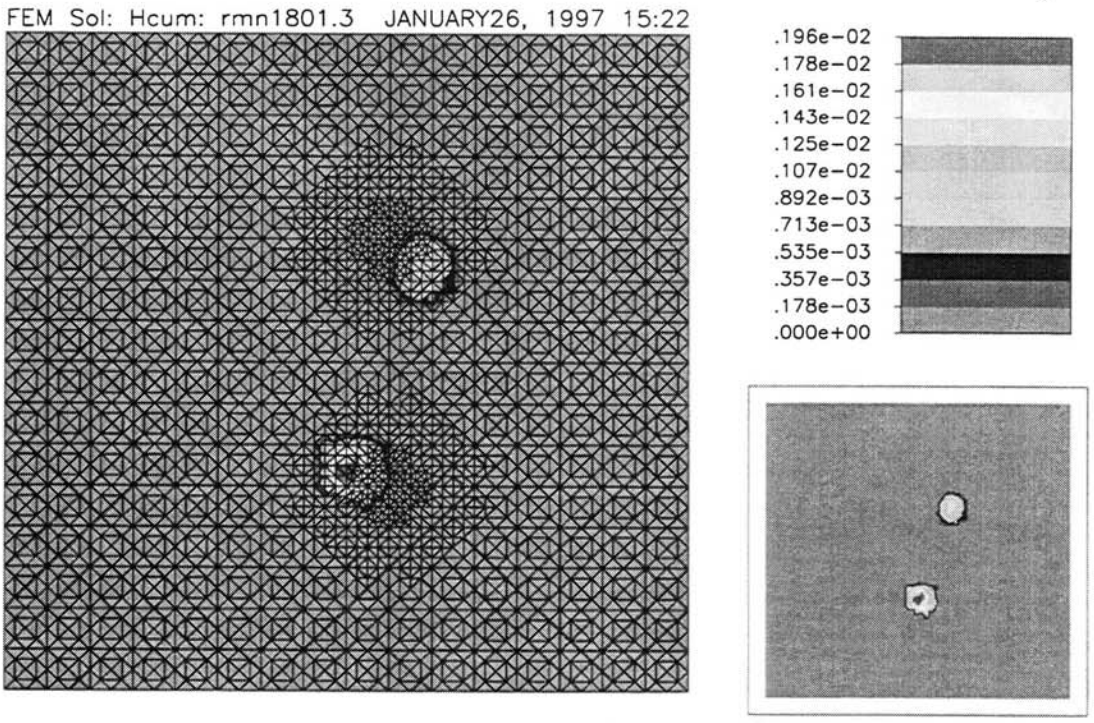

Figure 3. The final image for test #1 after 3 iterations

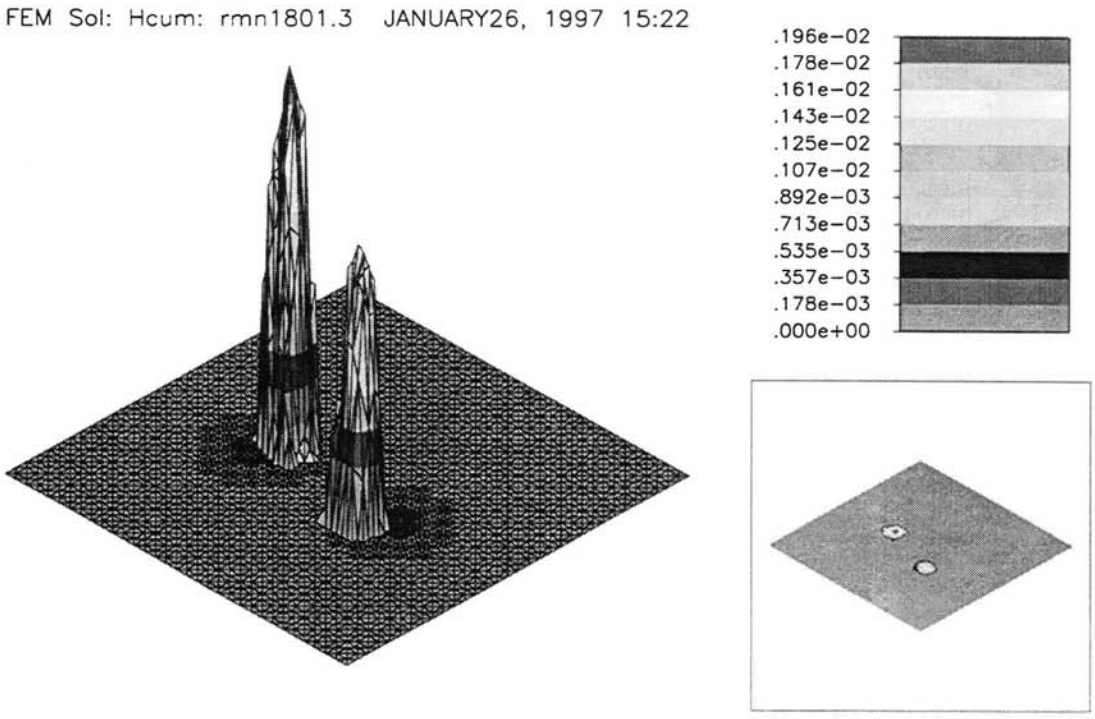

Figure 4. 3-Dimensional view of the image of Fig. 3

Test #2. In this test we introduced the above noise in the flux readings. The rest of the parameters were the same as in the first test. Figure 5 shows the image obtained on the first iteration of the ESM in 1.3 minutes CPU time (virtually real time). The inclusions are located accurately, and their separation is clear. Figure 6 displays the final image obtained in 4 minutes total CPU time after 3 iterations of the ESM. Figure 7 shows the 3-Dimensional view of this image. The locations of the inclusions are imaged more accurately than in the first test.

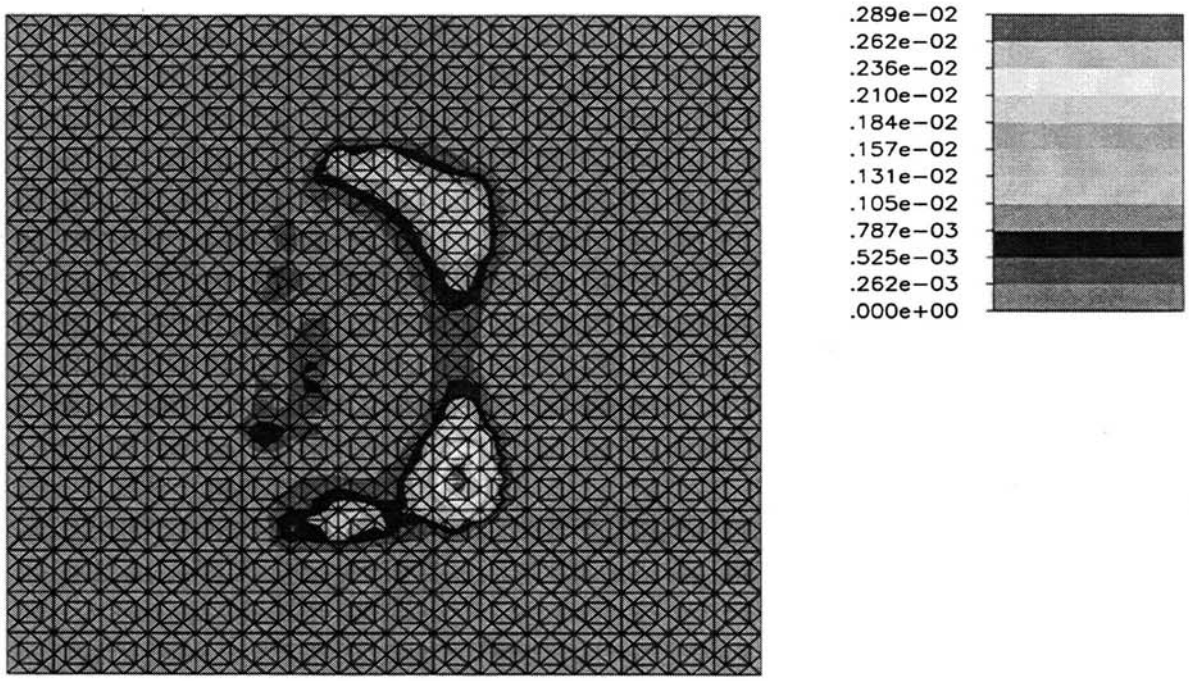

Figure 5. The image obtained on the first iteration for the test #2 in 1.3 minutes of CPU time

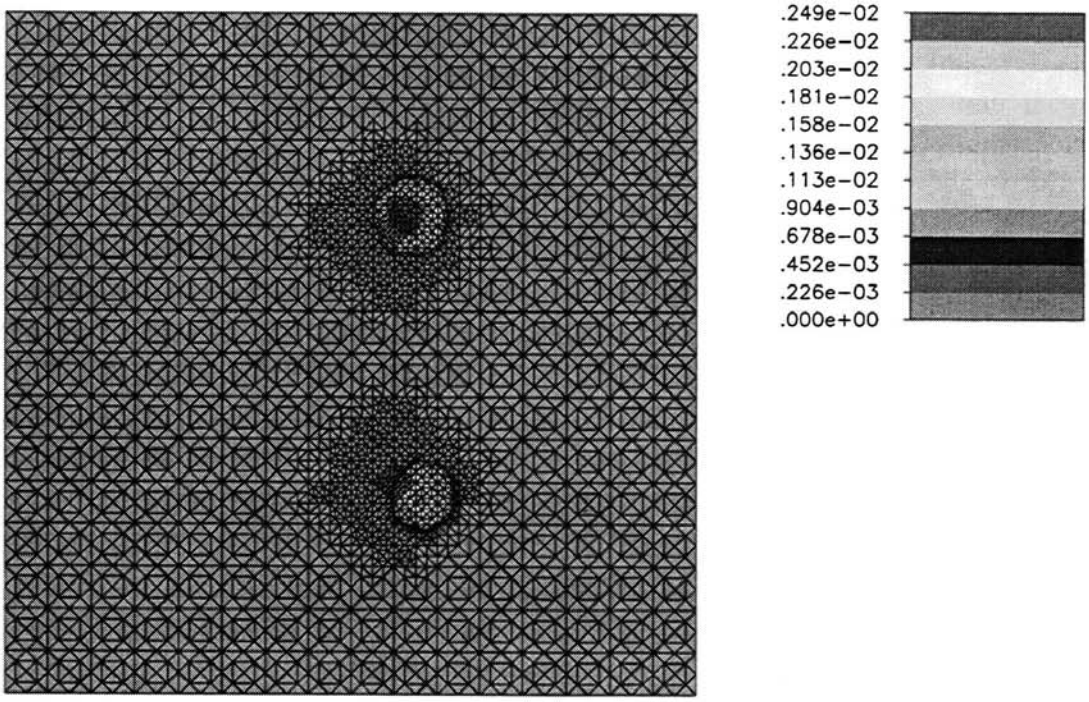

Figure 6. The final image for test #2 after 3 iterations

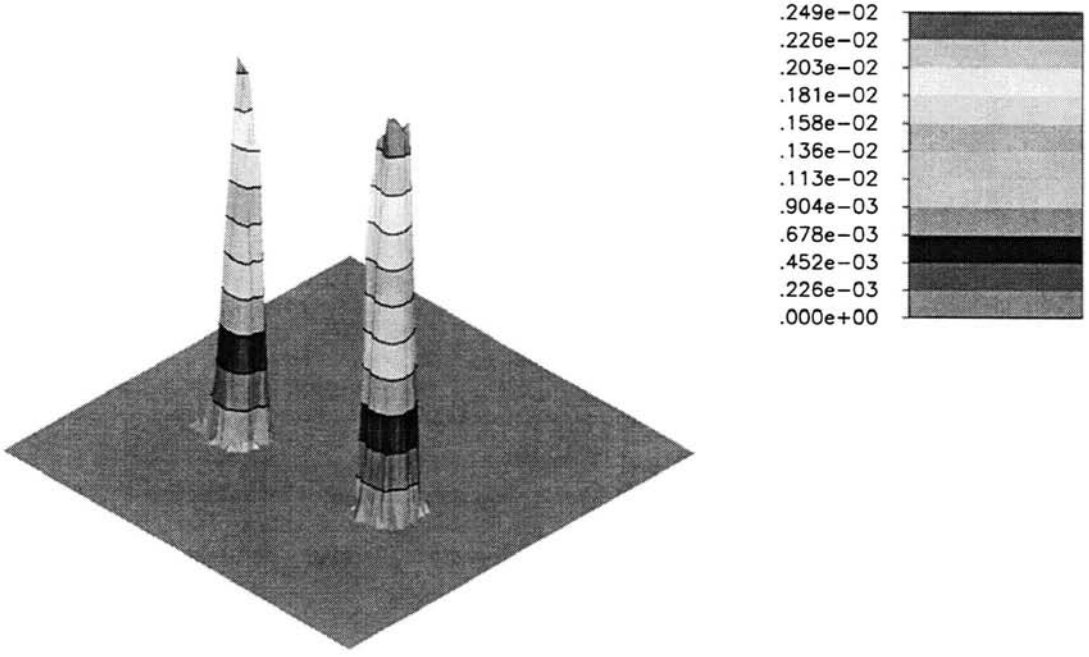

Figure 7. $3-D$ view of the image for Fig. 6

4. Conclusions

We have tested a novel numerical imaging algorithm [5] for diffusion/optical tomography in the time domain for the case of an anatomically accurate optical map of a female breast. The locations of small, low contrast "tumors" are imaged accurately. The accuracy of images is better in the case when the noise is introduced in the flux readings. This suggests that collimated detectors might be more advantageous than uncollimated ones.

This novel numerical method is very fast: it gives a good guess about abnormalities in almost real time, and the final image can be obtained in 4 minutes of CPU time total, with no pre-computations. This is orders of magnitude faster than in existing techniques, c.f. [1-3,8].

It is also important to note that the ESM can be applied to measurement schemes other than the time domain, such as AC and DC measurements [6]. This, as well as the high speed and accuracy of the ESM lead us to believe that this approach has the potential to become a *practically* valuable imaging algorithm, or adjunct.

ACKNOWLEDGMENTS

This research was supported in part by a Faculty Support Program grant from the University of North Carolina at Charlotte, by the National Science Foundation under grant No. DMS-9508414 (computing resources), and by NIH grant R01 CA59955.

REFERENCES

1. S. Arridge and M. Schweiger, 1995, Sensitivity to prior knowledge in optical tomographic reconstruction, *Proc. of SPIE*, **2389,** 378-388.

2. R. Barbour, H. Graber, J. Chang, S. Barbour, S. Koo, and R. Aronson, MRI-guided optical tomography, *IEEE Comp. Sci. Eng.*, **2**, #4, 63-77, 1995.

3. W. Cai, B. Das, F. Liu, M. Zevallos, M. Lax, and R. Alfano, Time-resolved optical diffusion tomographic image reconstruction in highly scattering turbid media, *Proc. Natl. Acad. Sci. USA*, **93**, 13561-13564, 1996.

4. C. Johnson, *Numerical Solution of Partial Differential Equations By The Finite Element Method*, Cambridge University Press, New York, 1987.

5. M. Klibanov, T. Lucas, and R. Frank, New imaging algorithm in diffusion tomography, current proceedings.

6. M.V. Klibanov and T.R. Lucas, Method and apparatus for detecting and abnormality within a host medium, United States patent application; patent's assignee: University of North Carolina at Charlotte, 1997.

7. T. Lucas and H. Oh, The method of auxiliary mapping for the finite element solutions of elliptic problems containing singularities, *J. Comput. Phys.*, **1081**, pp. 327-342, 1993.

8. M. O'Leary, D. Boas, B. Chance, and A. Yodh, Images of inhomogeneous turbid media using diffuse photon density waves, in *Optical Society of America Proc. " Advances In Optical Imaging And Photon Migration"*, **21**, 106-115, 1994.